Hindawi
Journal of Chemistry
Volume 2018, Article ID 8623020, 7 pages
https://doi.org/10.1155/2018/8623020

Research Article

Experimental Investigation on CO_2 Injection in Block M

Peng Chen,[1,2] Linlin Wang,[3] Sidun Zhang,[4] Junqiang Fan,[5] and Song Lu[6]

[1]*Hubei Cooperative Innovation Center of Unconventional Oil and Gas, Yangtze University, Wuhan, Hubei 430100, China*
[2]*College of Earth Science, Yangtze University, Wuhan, Hubei 430100, China*
[3]*MLR Key Laboratory of Saline Lake Resources and Environments, Institute of Mineral Resources, CAGS, Beijing 100037, China*
[4]*CBM Company, PetroChina, Beijing 100028, China*
[5]*Well Testing Company, Bohai Drilling Company, PetroChina, Langfang 065000, China*
[6]*Production Logging Center of Logging Co. Ltd., PetroChina, Xi'an 710201, China*

Correspondence should be addressed to Linlin Wang; wanglinlin2003@sina.cn

Received 20 March 2018; Accepted 20 May 2018; Published 26 June 2018

Academic Editor: Mohamed Azaroual

The purpose of this report was to perform an experimental evaluation of enhanced oil recovery (EOR) using CO_2 injection. A slim tube test and PVT experiment are used to determine the minimum miscibility pressure as well as a few related physical properties. Combined with a long core displacement experiment and nuclear magnetic resonance, CO_2 flooding and CO_2-water alternate flooding are simulated, and the displacement efficiency of different types of pores is evaluated. The results indicate that the minimum miscibility pressure is 32.6 MPa, and the CO_2 flooding is at near-miscible conditions at the current formation pressure. The CO_2 solubility of crude oil is large, and the crude oil has a strong expansion ability after the CO_2 injection, which is beneficial for improving the recovery of CO_2. The EOR of CO_2-water alternate flooding is 3.97% higher than that of continuous CO_2 flooding, and the EOR in the small and middle pores in the CO_2-water alternate flooding is clearly higher. These results will be relevant for the future development of Block M.

1. Introduction

Located in the abdomen of the Junggar Basin, Block M has a reservoir depth of approximately 3900 m, porosity of 13.52%, and permeability of 15.27 mD, and it can be categorized as a low porosity and low permeability reservoir. The formation experiences a long period of sedimentary cycles with strong planar and longitudinal heterogeneity, which occur initially for the delta front sediments and later for the former delta sediments [1, 2]. The oil reservoir is developed using water injection; however, the effects of water flooding are poor, and there are significant problems in the development process. Firstly, certain oil wells produce water rapidly after water injection, and the water content rises quickly, thus resulting in several wells being shut down because of high-water content. Secondly, the plane heterogeneity is strong, the state of each well is extremely different, and significant water channeling occurs. Lastly, the overall development effects are poor, the current recovery rate is only 15.6%, and the remaining reserves of the reservoir are large.

CO_2-enhanced oil recovery (EOR) has been used worldwide for more than 50 years [3, 4]. The most commonly used methods for EOR by CO_2 injection are CO_2-water alternate flooding, immiscible flooding, miscible flooding, and cyclic CO_2 injection [5, 6]. The mechanism of EOR by injecting CO_2 primarily includes a reduction in the viscosity of crude oil and expansion, vaporization, extraction, and improvement in the oil removal efficiency [7, 8]. Based on the production date of the CO_2 EOR project in the Jilin oilfield, reservoir pressure and wellhead injection pressure are the primary factors used to control the performance of wells, whereas gravity extraction and light/medium distillation extraction are the key mechanisms for enhancing oil recovery in tight reservoirs [9]. Yu et al. analyzed the EOR mechanism in tight oil reservoirs using a CO_2 huff and puff technology and verified its feasibility to increase the recovery in volume fracturing horizontal wells in the Bakken oilfield [10].

Table 1: Physical parameters of the core samples.

Number	Core number	Length (cm)	Diameter (cm)	Permeability (10^{-3} μm^2)	Porosity (%)
1	M1-1	7.646	2.51	28.152	14.11
	M1-2	7.563	2.5	12.667	13.81
	M1-3	7.782	2.51	7.141	12.52
	M1-4	7.675	2.51	4.710	12.79
2	M2-1	8.66	2.51	29.959	14.52
	M2-2	7.55	2.51	10.998	13.33
	M2-3	6.54	2.51	8.612	13.15
	M2-4	8.13	2.51	4.125	12.47

To prevent CO_2 from channeling in the high-permeability layer during a multilayer combined CO_2 injection, a reasonable plugging agent has been developed [11]. CO_2-water alternate flooding can reduce the gas breakthrough, thus improving the displacement efficiency. Furthermore, several field application results demonstrate that it can enhance recovery by 5%–10% [12]. By integrating an orthogonal array and Tabu technology to a genetic algorithm, the optimization of key parameters in CO_2 flooding, such as injection speed, slug size, and cycle time, is formed, and good results have been achieved in the field [13]. CO_2-EOR has been widely studied and proven successful in numerous oilfields. Additionally, it is a mature method to EOR technology, and it can be used as a technique to improve the development effects of the M reservoir to study certain mechanisms.

Nuclear magnetic resonance is widely applied to the study of pore throat distribution and flow characteristics of fluids in porous media [14–16]. It is difficult to evaluate the permeability of a tight reservoir, and thus, certain studies combine the pore throat characteristics with the relaxation time T_2 of the nuclear magnetic resonance to solve this problem [17]. To evaluate the residual oil distribution and effects of imbibition on oil recovery after water flooding, nuclear magnetic resonance can be used to monitor the distribution of the remaining oil in pore throat after various flooding [18]. The application of nuclear magnetic resonance is less in the CO_2-EOR [19, 20]. Nuclear magnetic resonance and core displacement are combined to study the change in oil saturation in different pore throats, and further revealed the EOR mechanism under CO_2 injection [6].

Based on a slim tube test, PVT experiment, and long core displacement experiment, this study analyzes the minimum miscibility pressure and physical property changes of oil and evaluates the effects of continuous CO_2 flooding and CO_2-water alternate flooding after water flooding. Using nuclear magnetic resonance, the oil content of different pore throats is observed during flooding, which can clarify the flow mechanisms of different pore throats. Furthermore, a basis for improving oil recovery by CO_2 injection is provided, which can also result in references for other development methods.

2. Experimental Materials

Oil samples and sandstone core samples are collected from the Block M. The properties of the core samples used in the experiments are listed in Table 1. To characterize the heterogeneity of the reservoir, long cores are assembled with different properties of the core samples. Based on the physical distribution between the injection wells and the production wells, the permeability of the long cores is gradually improved from the inlet to the outlet in this experiment. Table 2 lists the components of the crude oil sample. The crude oil used in this experiment is dehydrated crude oil, and its viscosity of crude oil is 0.708 MPa·s under the reservoir conditions of 104°C and 32 MPa. The type of formation water used is $NaHCO_3$. The synthetic brine has a salinity of 16253 mg/L and viscosity of 0.457 MPa·s under the reservoir conditions, and its mineralization composition is listed in Table 3. CO_2 is an industrial gas with a purity of 99.99%.

Table 2: Crude oil composition.

Composition	Mole percent
N_2	0.50
CO_2	0.61
C1	40.47
C2	4.44
C3	2.82
iC4	1.97
nC4	1.32
iC5	3.11
nC5	0.47
C6	1.25
C7	1.98
C8	3.43
C9	2.82
C10	2.80
C11+	32.00

Table 3: Brine ion compositions.

Ion	Mass concentration (mg/L)
Na^+ K^+	6034
Ca^{2+}	153.6
Mg^{2+}	17.7
HCO_3^-	906
Cl^-	8971.3
SO_4^{2-}	170.4

3. Fluid Physical Property Experiment

3.1. Slim Tube Test. The minimum miscibility pressure is the most important parameter used to determine miscible displacement in CO_2 flooding. The slim tube test is commonly used to determine the minimum miscibility

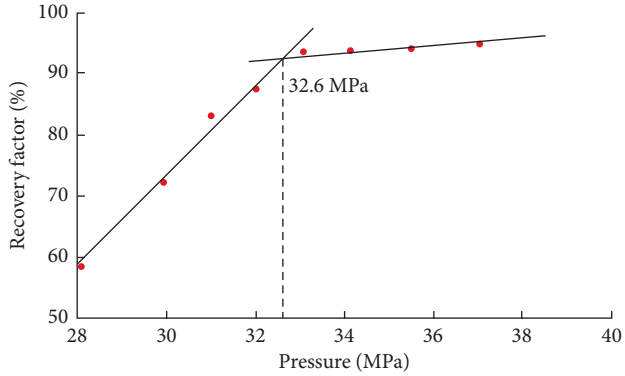

Figure 1: Recovery factor versus pressure to determine the minimum miscibility pressure.

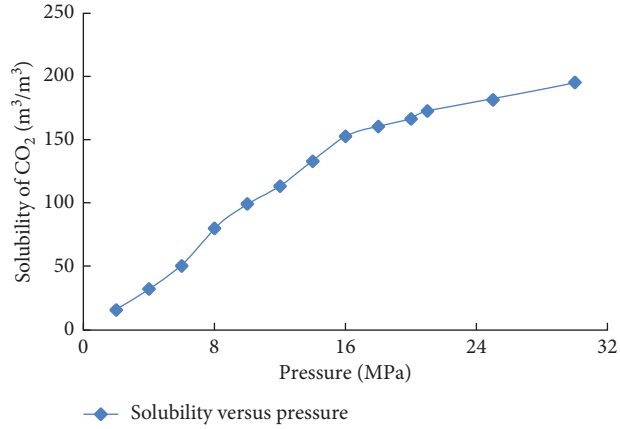

Figure 2: Curve of solubility versus pressure.

pressure [21]. The experiment is conducted at a temperature of 104°C. The length of the slim tube is 12.5 m with an inner diameter of 0.47 mm, and it is filled with quartz with a diameter of 140–230 μm. The porosity of the filling tube is 35%, the permeability is 5D, and the tube is saturated with crude oil, as indicated in Table 2. In this experiment, 1.2 PV of CO_2 is injected into the slim tube at a rate of 1 cm/min at 8 different pressures, and the oil recovery at different pressures is depicted in Figure 1. As the injection pressure increases, the oil recovery increases, and there is no apparent inflection point in this process. However, there is a gradual process, and the transition point from immiscible to miscible is at the near-miscible point. Based on the characteristics of the test points, the minimum miscibility pressure of Block M is 32.6 MPa, and the CO_2 injection point under the current reservoir condition occurs in the near-miscible flooding region.

3.2. PVT Experiment. The PVT characteristics of crude oil are closely related to the development effect in the CO_2 flooding [22, 23]. The PVT experiment is performed to understand the change in properties of the crude oil at the reservoir temperature. A CO_2 solubility experiment, including the viscosity of crude oil, is carried out to understand the change in properties of crude oil. During the CO_2 injection process, CO_2 dissolves in crude oil, oil volume increases, and viscosity decreases, which will make oil to flow out of pores. It is necessary to understand the solubility of CO_2 in crude oil and the change of viscosity, which will help to clarify the mechanism of CO_2-enhanced oil recovery.

The solubility of CO_2 in crude oil is an important parameter for immiscible flooding. A high-temperature and high-pressure sample (PY-1 type) is used, and the flash method is used to measure the solubility of CO_2 in the range of 2–30 MPa at 104°C. The result is shown in Figure 2. As the pressure increases, the solubility of CO_2 increases; however, it increases slowly after reaching a certain pressure. At 104°C, the solubility of CO_2 is 15.12 m^3/m^3 for 2 MPa and 195.27 m^3/m^3 for 30 MPa (Figure 2). This result indicates that the solubility in crude oil is large, and crude oil has a strong expansion ability during the CO_2 injection. Expansion of crude oil will cause some residual oil to be converted into mobile oil and increases the recovery rate.

Table 4: Oil viscosity.

Pressure (MPa)	Viscosity (MPa·s)		Decline percentage
	Normality	Dissolving CO_2	
0	0.708	0.708	0
5	0.712	0.655	7.49
10	0.715	0.559	21.05
15	0.718	0.542	23.45
20	0.722	0.513	27.54
25	0.724	0.497	29.80
30	0.726	0.489	30.93

When CO_2 is dissolved in the crude oil, the volume of the crude oil expands, whereas the viscosity decreases. To evaluate the change in viscosity during the CO_2 injection, the viscosity of the crude oil is tested at 104°C. The results indicate that the viscosity decreases significantly from 0.708 to 0.489 after dissolving CO_2 as the pressure increases from 0 MPa to 30 MPa (Table 4). The decrease in the viscosity of the crude oil reduces the mobility ratio between the fluids, and it can reduce the gas cone, improve the utilization efficiency of the injected gas, and enhance the oil recovery.

4. CO_2 Injection Experiment

4.1. Experimental Method. Ideally, the flooding experiment should use a natural long core; however, it is not feasibly obtained from the current coring technique. Currently, a natural short core is commonly used to assemble the long core in a certain arrangement. The permeability of the long core can be given as follows:

$$\frac{\overline{L}}{\overline{K}} = \frac{L_1}{K_1} + \frac{L_2}{K_2} + \cdots + \frac{L_i}{K_i} + \cdots + \frac{L_n}{K_n} = \sum_{i=1}^{n} \frac{L_i}{K_i}, \quad (1)$$

where $\overline{L}$ is the length of the long core, $\overline{K}$ is the permeability of the long core, L_i is the length of the short core i, and K_i is the permeability of the short core i.

The experimental device is primarily composed of the injection system, core holder system, and output measurement system (Figure 3). The injection system consists of

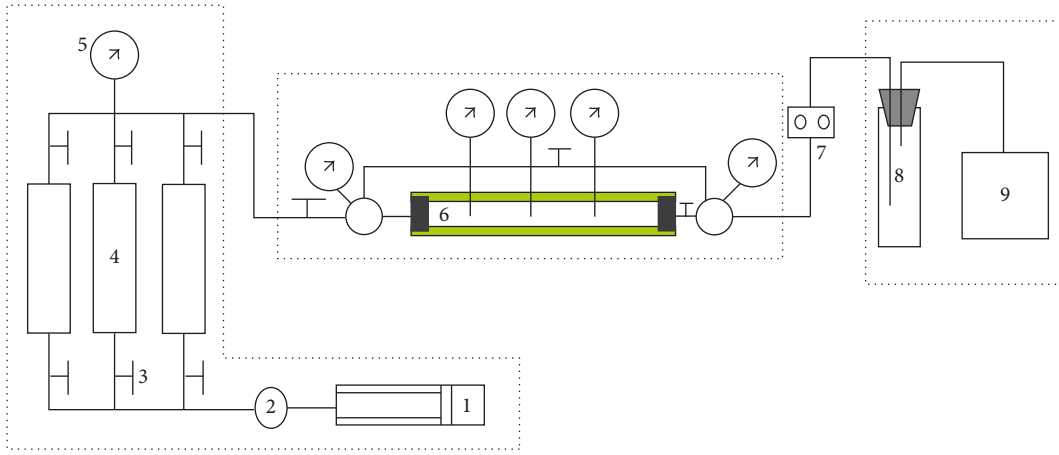

Figure 3: Experiment apparatus of CO_2 injection. 1: Liquid pump; 2: six-way valve; 3: valve; 4: gas and liquid container; 5: pressure gauge; 6: core holder; 7: backpressure controller; 8: separator; 9: gauging device.

an injection pump, fluid tube, and temperature control device. The core holder system includes a core holder, thermostat, and pressure control device. The output measurement system is comprised of a three-phase separator and gauging device.

The CO_2 flooding experiment and CO_2-water alternate flooding experiment are designed to evaluate the effects of CO_2 EOR at Block M. In this experiment, the temperature is controlled at 104°C, and the displacement rate is 0.125 cm^3/min. The experimental procedure can be briefly described as follows: (1) certain basic parameters of the short cores are measured; (2) the long core is assembled, vacuumed for 12 h, and saturated with synthetic brine water under 10 MPa for 24 h; (3) the irreducible water is established through oil flooding, the irreducible water saturation is calculated, and the sample rests for 24 h; (4) the sample is displaced by water until the water is reduced by 98%, CO_2 is then used for displacement, and the experiment is terminated when the oil production no longer increases; and (5) the other sample repeats the above process, and CO_2-water alternate flooding is conducted after the water flooding. The volume ratio of water to gas is 1 : 1.

4.2. Relationship between the Relaxation Time T_2 and the Pore Throat Radius. Nuclear magnetic resonance is primarily used as a signal to detect the hydrogen nuclear atom, and it analyzes the distribution of fluid in different pore throats. Using heavy water as the water phase, the signal is not generated when the relaxation time T_2 is measured. The T_2 spectrum is T_2 of the oil phase in the core. The T_2 spectrum before displacement reflects the occurrence of crude oil in the original state, and the T_2 spectrum after displacement reflects the remaining oil. The change in the T_2 spectrum can quantitatively analyze the degree of oil production, remaining oil occurrence, and displacement potential, and it can provide guidance for development of the potential evaluation and program adjustment.

The distribution curves of the relation time T_2 can reveal the distribution of the pore throat, and a correlation exists. Due to the complexity and irregularity of the pore throat, its surface area and volume ratio are avoided. In the actual calculation, the surface relaxation rate of ρ_2 and the structure factor F_S is used as the conversion factor. The expression of the relaxation time T_2 and the pore throat radius r can be written as follows [24]:

$$\frac{1}{T_2} = \rho_2 \frac{F_s}{r}. \tag{2}$$

The relaxation time T_2 distribution represents a complex geometrical arrangement including small to large pore size domains [25, 26]. The relaxation time T_2 is less than 10 ms, which is equivalent to the pore size of clay. From 10 ms to 100 ms, the pore is mesoporous. When T_2 is greater than 100 ms, the pore is macroporous [6, 27]. The relationship between the percentage of volume distribution and the relaxation time T_2 is used to reveal the degree of oil production in different pore throats and describe the displacement mechanism and the remaining oil distribution.

5. Results and Discussion

In order to evaluate the effect of CO_2 flooding and CO_2-water alternate flooding, they are used to continue to displace the core after water flooding. The T_2 spectrum is T_2 of the oil phase in the core, it shows the amount of remaining oil in the pores of different sizes, and the T_2 spectrum frequency of the pores decreases when oil is extracted from the pores. If the frequency distribution of the T_2 spectrum is obtained after water flooding, CO_2 flooding, and CO_2-water alternate flooding, the degree of recovery of oil in different pores can be analyzed under these flooding methods. Two sets of core displacement experiments are conducted, CO_2 flooding and CO_2-water alternate flooding are used, respectively, after water flooding, and the frequency distribution of T_2 spectrum is monitored after these experiments.

When the rate of water content is increased to 98%, the injection of water in sample no. 1 is terminated. The recovery factor is 50.17%, and the sample is scanned using nuclear magnetic resonance. Then, CO_2 flooding is performed, and the displacement is terminated without apparent oil recovery, resulting in a recovery rate of 58.91%, Then, the core is rescanned, and the recovery rate of the CO_2 flooding

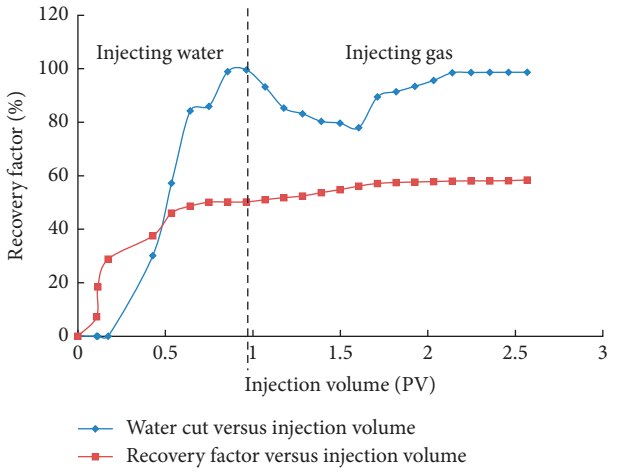

Figure 4: Curve of the recovery factor during continuous CO_2 flooding after water flooding.

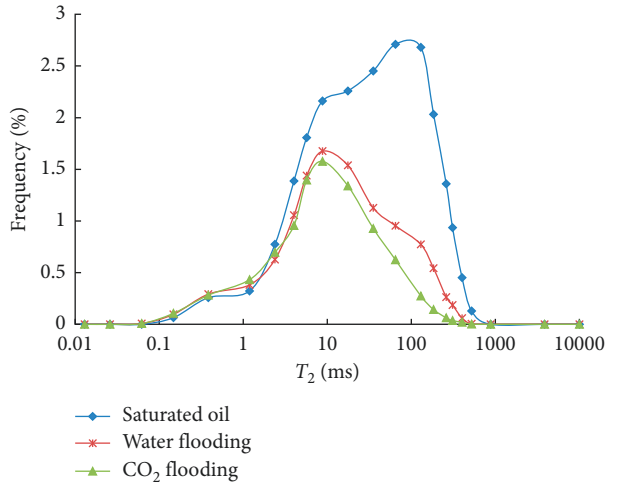

Figure 5: Distribution of residual oil with T_2 during CO_2 flooding.

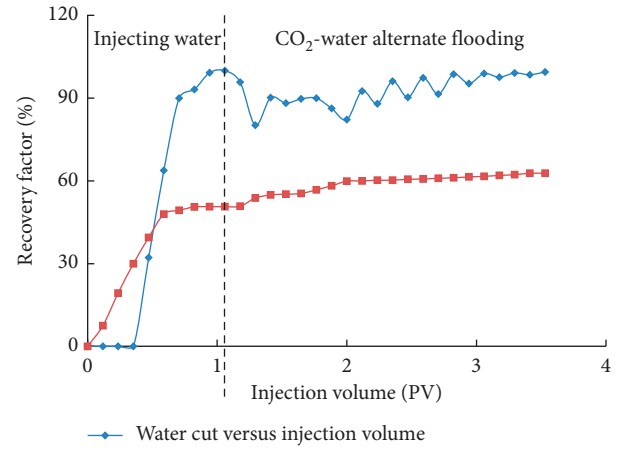

Figure 6: Curve of the recovery factor during CO_2-water alternate flooding after water flooding.

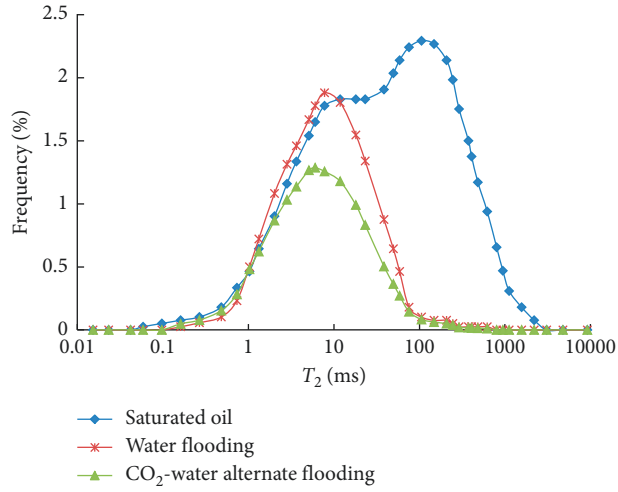

Figure 7: Distribution of residual oil with T_2 during CO_2-water alternate flooding.

increases by 8.74%. At the beginning of the water flooding process, the sample is purely oil-extracted, and the recovery of oil significantly increases and then decreases with an increase in the water content. During the CO_2 flooding, the volume of oil expands after dissolving CO_2 and part of immovable oil becomes movable, oil production increases, and the water content decreases significantly and then increases slowly (Figure 4). Because the oil in some channels is produced after flooding, the frequency of the T_2 spectrum decreases in these channels. The curve of the relation time T_2 shows that the oil in the large and medium pores has a high degree of recovery, and the crude oil in the small pores has not been used during the water flooding process. After the CO_2 flooding, the crude oil production in the large and medium pores is further improved, whereas the oil recovery in the small pores remained nearly unchanged (Figure 5). This may be due to the relatively small flow resistance in large and medium pores, which forms a dominant percolation channel.

Water is injected to a water content of 98%, and the water flooding process is then stopped in sample no. 2, resulting in a recovery factor of 50.66%. Then, the sample is scanned. Next, CO_2-water alternate flooding is performed, and the flooding is terminated when there is no significant oil recovery, resulting in a recovery factor of 62.88%. Lastly, the core is scanned again. The CO_2-water flooding enhances the recovery rate by 12.22%. In the displacement process, the recovery of oil is almost similar to that of sample no. 1, and the water content increases in a wave-like manner during the CO_2-water alternating flooding process (Figure 6). In the process of water flooding, the degree of oil recovery in the large-medium pores is high, the oil in the large pores is basically produced, and the oil in the small pores is not used. The large-medium pores form a dominant percolation channel during the water flooding, and capillary force makes it difficult to flow in the small pores. After the CO_2-water alternating flooding occurs, the capillary force between two phases of gas and water is larger, displacement pressure increases at both ends of the pores, oil begins to flow in small pores, and the oil in the small pores significantly increases (Figure 7).

In the process of CO_2 flooding and CO_2-water alternating flooding, the difference in the displacement mechanism may cause a significant difference in the oil recovery rate in the small pores. The EOR of CO_2 flooding in this experiment occurs primarily due to these facts: CO_2 is dissolved in crude oil to cause expansion of crude oil, which increases the saturation of the oil phase in the pores, and part of the irreversible oil becomes movable oil. The interfacial tension between oil and CO_2 is small in near-mixed conditions, and gas can displace crude oil in the small pores. Additionally, extraction can improve oil recovery to a certain extent. CO_2-water alternate flooding involves the EOR mechanism of CO_2 flooding. Furthermore, the interfacial tension between the gas phase and the water phase is large, thus resulting in a large capillary force and avoiding the formation of gas flow advantage channels, which can improve the oil output in the small pores and enhance oil recovery.

6. Conclusion

Based on the slim tube test, PVT experiment, and flooding experiment of the long core, the miscible pressure of Block M is determined, the feasibility of CO_2 injection to enhance oil recovery is evaluated, and nuclear magnetic resonance is combined to analyze the recovery of oil in different sizes of pore throats. A few conclusions can be drawn as follows: the miscible pressure of Block M is 32.6 MPa, and the CO_2 flooding approaches miscible flooding under the current formation condition. The oil recovery can reach 58.9% when using CO_2 flooding after water flooding, which is an improvement of 8.74%. The recovery using CO_2-water alternate flooding after water flooding reaches 62.88%, which is an increase of 12.22%. This result demonstrates that the effects of CO_2-water alternate flooding are superior. Medium and large pores have a high displacement efficiency, and the efficiency of the small pore displacement is extremely low during the water flooding process. CO_2 flooding primarily increases the displacement efficiency in macropores and mesopores; however, CO_2-water alternate flooding can also increase the displacement efficiency of small pores. These results are significant for improving the development effects of Block M.

Data Availability

The raw data used to support the findings of this study are available from the corresponding author upon request.

Conflicts of Interest

The authors declare that they have no conflicts of interest.

Acknowledgments

This work was supported by the Science and Technology Research Project of Hubei Provincial Department of Education (Grant nos. B2017035 and Q20171301).

References

[1] S. Li, L. Liu, Y. Zhang et al., "Sedimentary evolution and microfacies architecture of the Jurassic Sangonghe formation in Mobei Arch, Junggar Basin," *Acta Sedmentologica Sinica*, vol. 24, no. 6, pp. 819–828, 2006.

[2] Y. Pan, C. Zhang, Q. Wu, S. Hou, Q. Ma, and M. Ji, "CO_2 displacing mechanism and optimized design of the development feasibility for Sangong-River low-permeability oil reservoirs," *Petroleum Geology and Oilfield Development in Daqing*, vol. 36, no. 1, pp. 124–128, 2017.

[3] R. M. Enick, D. K. Olsen, J. R. Ammer, and W. Schuller, "Mobility and conformance control for CO_2 EOR via thickeners, foams, and gels—a literature review of 40 years of research and pilot tests," in *Proceedings of the SPE Improved Oil Recovery Symposium*, Tulsa, OK, USA, April 2012.

[4] S. Ghedan, "Global laboratory experience of CO_2-EOR flooding," in *Proceedings of the SPE/EAGE Reservoir Characterization and Simulation Conference*, Abu Dhabi, UAE, October 2009.

[5] M. Riazi, M. Sohrabi, and M. Jamiolahmady, "Experimental study of pore-scale mechanisms of carbonated water injection," *Transport in Porous Media*, vol. 86, no. 1, pp. 73–86, 2011.

[6] P. Xiao, Z. Yang, X. Wang, H. Xiao, and X. Wang, "Experimental investigation on CO_2 injection in the Daqing extra/ultra-low permeability reservoir," *Journal of Petroleum Science and Engineering*, vol. 149, pp. 765–771, 2017.

[7] E. A. Chukwudeme and A. A. Hamouda, "Enhanced oil recovery (EOR) by miscible CO_2 and water flooding of asphaltenic and non-asphaltenic oils," *Energies*, vol. 2, no. 3, pp. 714–737, 2009.

[8] A. A. Alquriaishi and E. M. E.-M. Shokir, "Experimental investigation of miscible CO_2 flooding," *Petroleum Science and Technology*, vol. 29, no. 19, pp. 2005–2016, 2011.

[9] B. Ren, S. Ren, L. Zhang, G. Chen, and H. Zhang, "Monitoring on CO_2 migration in a tight oil reservoir during CCS-EOR in Jilin oilfield China," *Energy*, vol. 98, pp. 108–121, 2016.

[10] W. Yu, H. R. Lashgari, K. Wu, and K. Sepehmoori, "CO_2 injection for enhanced oil recovery in Bakken tight oil reservoirs," *Fuel*, vol. 159, no. 1, pp. 354–363, 2015.

[11] F. Li, Y. Luo, X. Lou, L. Wang, and R.D. Nagre, "Experimental study on a new plugging agent during CO2 flooding for heterogeneous oil reservoirs: a case study of Block G89-1 of Shengli oilfield," *Journal of Petroleum Science and Engineering*, vol. 146, pp. 103–110, 2016.

[12] J. R. Christensen, E. H. Stenby, and A. Skauge, "Review of WAG field experience," in *Proceedings of the International Petroleum Conference and Exhibition of Mexico*, Villahermosa, Mexico, March 1998.

[13] S. Chen, H. Li, D. Yang, and P. Tontiwachwuthikul, "Optimal parametric design for water-alternating-gas (WAG) process in a CO_2-miscible flooding reservoir," *Journal of Canadian Petroleum Technology*, vol. 49, no. 10, pp. 75–82, 2010.

[14] W. Looyestijin and J. Hofman, "Wettability-index determination by nuclear magnetic resonance," *SPE Reservoir Evaluation and Engineering*, vol. 9, no. 2, pp. 146–153, 2006.

[15] H. Daigle and B. Dugan, "Extending NMR data for permeability estimation in fine-grained sediments," *Marine and Petroleum Geology*, vol. 26, no. 8, pp. 1419–1427, 2009.

[16] Q. Zhang, Y. H. Dong, S. Q. Tong, L. I. Xiao, and L. H. Wang, "Nuclear magnetic resonance cryoporometry as a tool to measure pore size distribution of shale rock," *China Science Buletin*, vol. 61, no. 21, pp. 2387–2394, 2016.

[17] R. Rezaee, A. Saeedi, and B. Clennell, "Tight gas sands permeability estimation from mercury injection capillary pressure and nuclear magnetic resonance data," *Journal of Petroleum Science and Engineering*, vol. 88-89, no. 2, pp. 92–99, 2012.

[18] C. Xu, H. Liu, G. Qian, and J. Qin, "Microcosmic mechanisms of water-oil displacement in conglomerate reservoirs in Karamay Oilfield, NW China," *Petroleum Exploration and Development*, vol. 38, no. 6, pp. 725–732, 2011.

[19] T. Suekane, N. Furukawa, S. Tsushima, S. Hirai, and M. Kiyoto, "Application of MRI in the measurement of two-phase flow of supercritical CO_2 and water in porous rocks," *Journal of Porous Media*, vol. 12, no. 12, pp. 143–154, 2009.

[20] A. Z. Al-yaseri, Y. Zhang, M. Ghasemiziarani et al., "Permeability evolution in sandstone due to CO_2 injection," *Energy and Fuels*, vol. 31, no. 11, pp. 12390–12398, 2017.

[21] A. H. Fath and A. R. Pouranfard, "Evaluation of miscible and immiscible CO_2, injection in one of the Iranian oil fields," *Egyptian Journal of Petroleum*, vol. 23, no. 3, pp. 255–270, 2014.

[22] M. Ding, X. A. Yue, H. Zhao, and W. Zhang, "Extraction and its effects on crude oil properties during CO_2 flooding," *Energy Sources, Part A: Recovery, Utilization, and Environmental Effects*, vol. 35, no. 23, pp. 2233–2241, 2013.

[23] M. Seyyedi, P. Mahzari, and M. Sohrabi, "A comparative study of oil compositional variations during CO_2, and carbonated water injection scenarios for EOR," *Journal of Petroleum Science and Engineering*, vol. 164, pp. 685–695, 2018.

[24] J. Gong, S. Liu, M. Zhao, H. Xie, and K. Liu, "Characterization of micro pore throat radius in tight oil reservoirs by NMR and high pressure distribution mercury injection," *Petroleum Geology and Experiment*, vol. 38, no. 3, pp. 389–394, 2016.

[25] A. Dillinger and L. Esteban, "Experimental evaluation of reservoir quality in Mesozoic formations of the Perth Basin (Western Australia) by using a laboratory low field nuclear magnetic resonance," *Marine and Petroleum Geology*, vol. 57, no. 2, pp. 455–469, 2014.

[26] A. F. Li, X. X. Ren, G. J. Wang, and K. Jiang, "Characterization of pore structure of low permeability reservoir using a nuclear magnetic resonance method," *Journal of China University of Petroleum*, vol. 39, no. 6, pp. 92–98, 2015.

[27] J. Lai, G. Wang, J. Cao et al., "Investigation of pore structure and petrophysical property in tight sandstones," *Marine and Petroleum Geology*, vol. 91, pp. 179–189, 2018.